nature climate change

SUPPLEMENTARY INFORMATION

DOI: 10.1038/NCLIMATE1331

Microbial mediation of carbon-cycle feedbacks to climate warming

Jizhong Zhou[1,2,3,4], Kai Xue[1,2], Jianping Xie[1,2,5], Ye Deng[1,2], Liyou Wu[1,2], Xiaoli Cheng[2], Shenfeng Fei[2], Shiping Deng[6], Zhili He[1,2], Joy D. Van Nostrand[1,2], and Yiqi Luo[2]

[1]*Institute for Environmental Genomics, and* [2]*Department of Botany and Microbiology, University of Oklahoma, Norman, OK 73019, USA*

[3]*Earth Science Division, Lawrence Berkeley National Laboratory, Berkeley, CA, 94270, USA*

[4]State Key Joint Laboratory of Environment Simulation and Pollution Control, School of Environment, Tsinghua University, Beijing 100084, China.

[5]*School of mineral processing and bioengineering, Central South University, Changsha, Hunan, 410083, China*

[6]*Department of Plant and Soil Sciences, Oklahoma State University, Stillwater, OK 74078, USA*

Supp Tables: Supplementary Tables, pdf file, 18k

Supp Figures: Supplementary Figures, pdf file, 315k

Supp Materials and Methods: Supplementary Materials and Methods, pdf file, 243k

Supp Text: Supplementary Text, pdf file, 103k

SUPPLEMENTARY TABLES

Table. **S1**. Warming induced C_4 derived-carbon (C) increases (%, mean ± standard error, n=6) in light fraction (LF), intra-aggregate particulate organic matter (iPOM) and mineral soil organic matter (mSOM) of different aggregate size classes. The significance of the increase was tested by two-tailed t tests. Asterisks indicate $p < 0.05$ (**) and $p < 0.10$ (*).

Fractions by size	Fraction by density	Warming induced C increase (%)
>2000 μm	LF	16.44 ± 4.92**
	iPOM	5.42 ± 5.86
	mSOM	7.76 ± 5.67
2000-250 μm	LF	11.28 ± 8.10
	iPOM	8.65 ± 4.83
	mSOM	9.21 ± 4.08*
250-53 μm	LF	5.60 ± 2.47
	iPOM	4.44 ± 2.91
	mSOM	6.14 ± 3.34

Table S2. Overall microbial community diversity detected by GeoChip and pyrosequencing under warming and the control (mean ± standard error, n=6 for functional genes and 15 for 16S rRNA gene).

Dataset	Detected gene number			Inverse Simpson Index (1/*D*)		
	Warming	Control	P[a]	Warming	Control	P[a]
Functional genes	999±194[b]	728±180[b]	0.16	993.45±192.90	724.43±179.52	0.16
16S rRNA gene	1837±510[c]	1808±742[c]	0.920	523.60±144.58	495.02±125.48	0.565

[a] p-value of two-tailed paired t test;
[b]Total functional gene number;
[c]Total OTU number.

SUPPLEMENTARY FIGURES

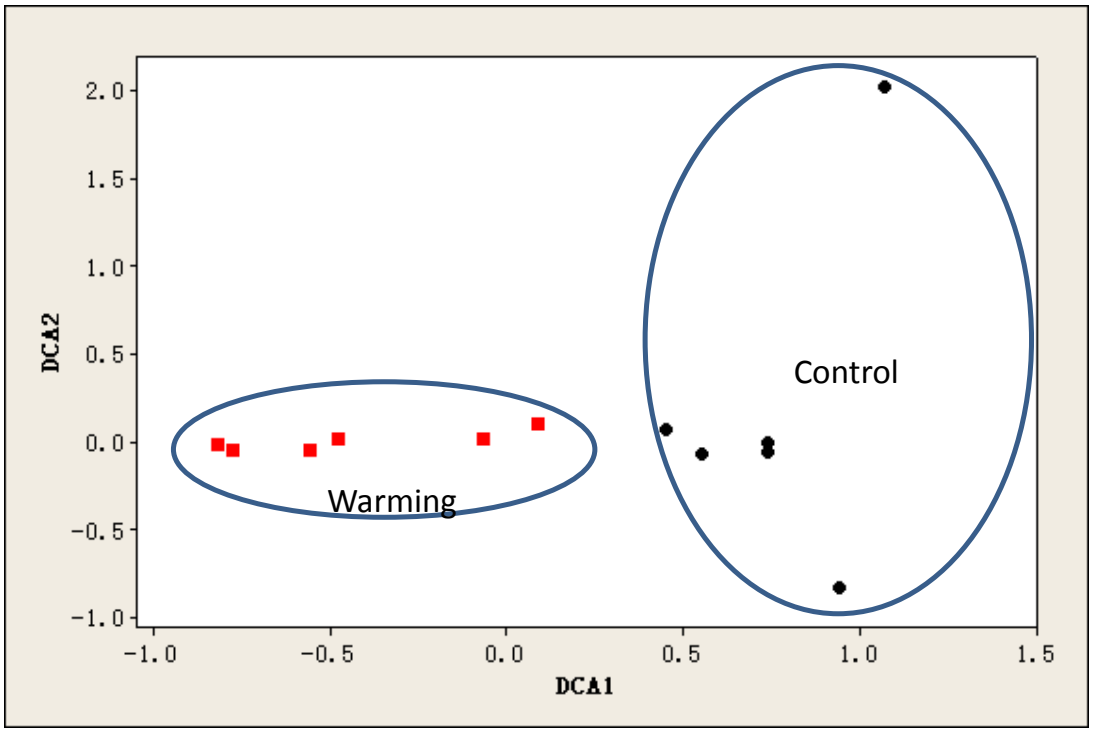

Fig. S1. Detrended correspondence analysis (DCA) of GeoChip data showing that warming significantly altered the soil microbial community composition and functional structure. The effects of warming on the soil microbial community composition and structure were well separated by DCA1.

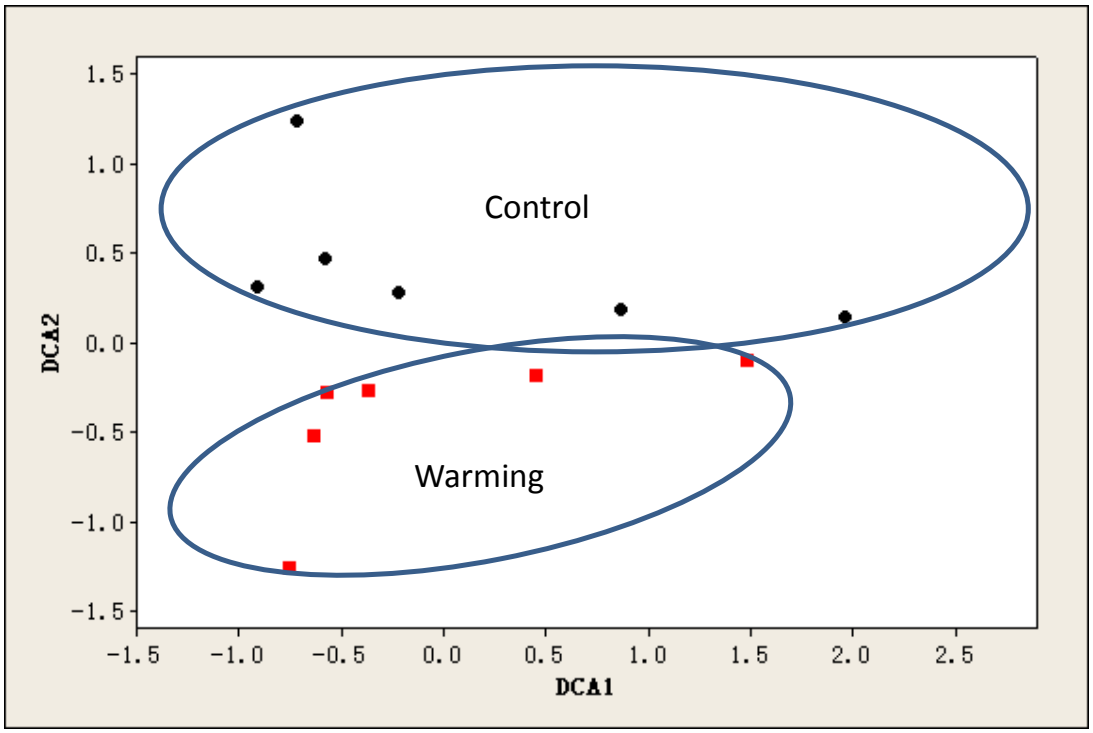

Fig. S2. Detrended correspondence analysis (DCA) of pyrosequencing data showing that warming significantly affected the soil microbial community composition. The effects of warming on the soil microbial community composition and structure appeared to be well separated by the DCA2.

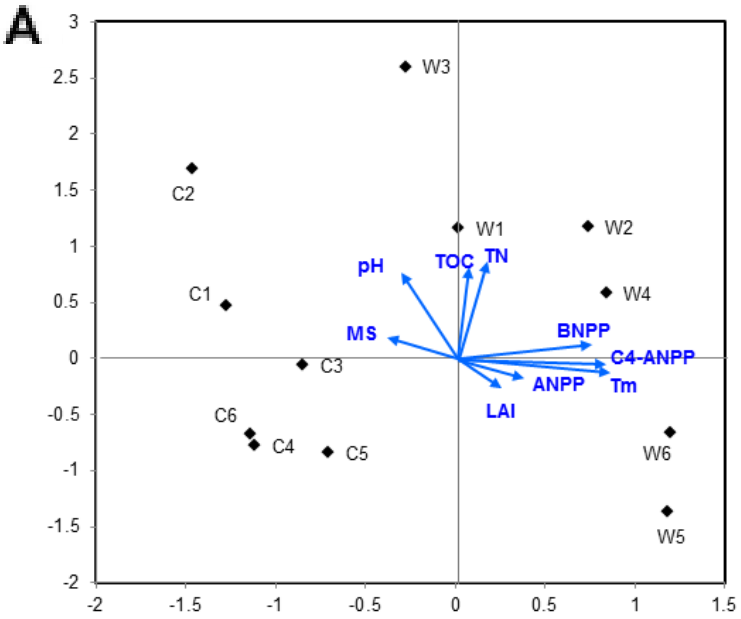

	F	*p*
Soil	1.232	0.039
pH	1.382	0.056
TOC	1.143	0.196
TN	1.235	0.128
Plant	1.189	0.033
C4-ANPP	1.685	0.008
LAI	1.061	0.312
BNPP	1.578	0.034
ANPP	1.023	0.356
Tm & MS	1.431	0.005
Tm	1.894	0.001
MS	1.033	0.351
Whole	1.190	0.025

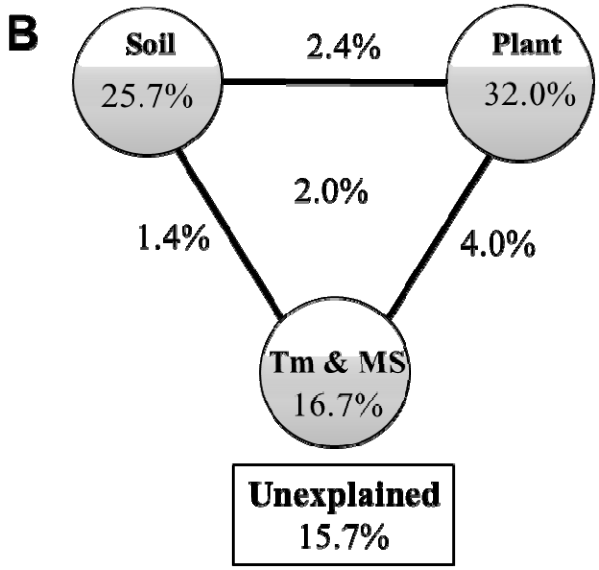

Fig. S3. Constrained ordination analysis. (A) Canonical correspondence analysis (CCA) of GeoChip data and environmental variables, which showed that microbial community functional composition and structure were significantly shaped by several key environmental factors: leaf area index (LAI), belowground net primary productivity (BNPP), aboveground net primary productivity (ANPP), C_4 net primary productivity (C_4-ANPP), soil temperature (Tm), moisture (MS), pH, total organic C (TOC) and N (TON). C1 – C6 refer control plots without warming, whereas W1-W6 represent the plots under warming. The insert table showed the significances of each or subsets of the environmental variables in explaining the variations of microbial community functional gene

structure based on F-test. (**B**) CCA-based variation partitioning analysis (VPA) which showed the relative proportions of community structure variations that can be explained by different types of environmental factors. The circles show the variation explained by each group of environmental factors alone. The numbers between the circles show the interactions of the two factors on either side and number in the center of the triangle represents interactions of all three factors.

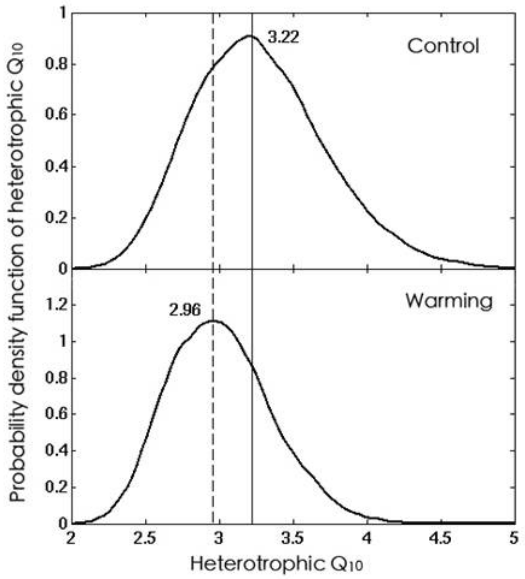

Fig. S4. The marginal distribution of modeled Q_{10} values for heterotrophic soil respiration in control plots (solid line) and warming plots (dashed line). The best estimation of Q_{10} is lower in warmed plots than that in control plots. The inverse analysis of Q_{10} was performed in a revised Terrestrial ECOsystem (TECO) model by the Markov Chain Monte Carlo (MCMC) method. In each treatment condition, 20,000 Q10 values were inversely estimated. The figure here shows the probability density of the Q_{10} values for each treatment with the assumption that the best estimation of Q_{10} has the highest probability density.

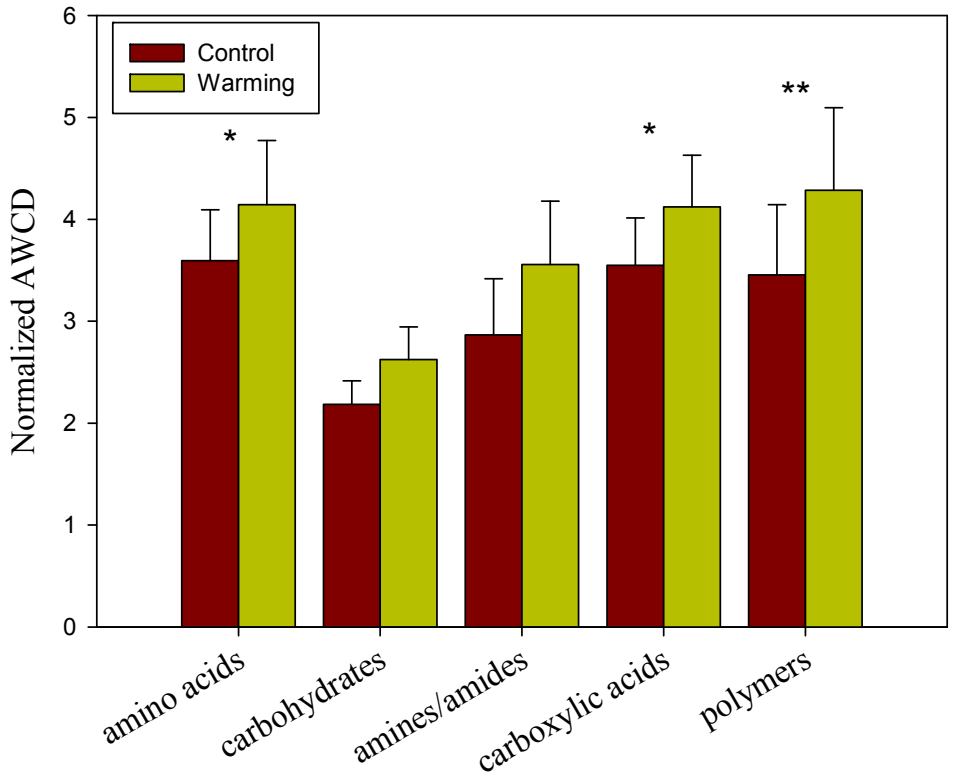

134

135 **Fig. S5.** The normalized average well color development (AWCD) for soil samples incubated for 48
136 h by BIOLOG ECO MICROPLATE to measure the substrate utilization profiles of soil microbial
137 communities under warming and control. Error bars indicate standard error of the data (n=6). The
138 differences between warming and the control were tested by two-tailed paired t-tests and labeled
139 with ** when $p < 0.05$, and * when $p < 0.10$.

140

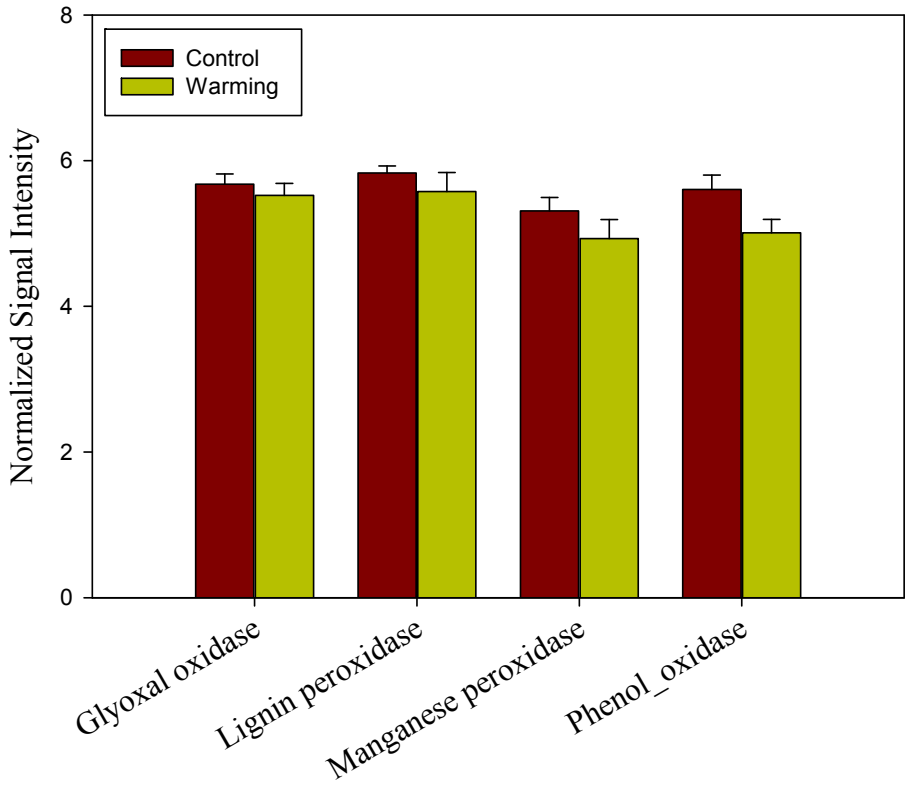

141

142 **Fig. S6.** The normalized average signal intensity of detected genes involved in lignin degradation
143 under warming and the control in 2008. The signal intensities were the average abundances of
144 detected genes from warming or control plots, normalized by the probe number for each gene. Error
145 bars indicate standard error of the data (n=6). The differences between warming and control were
146 tested by two-tailed paired t-tests and none shows a statistically significantly difference.

147

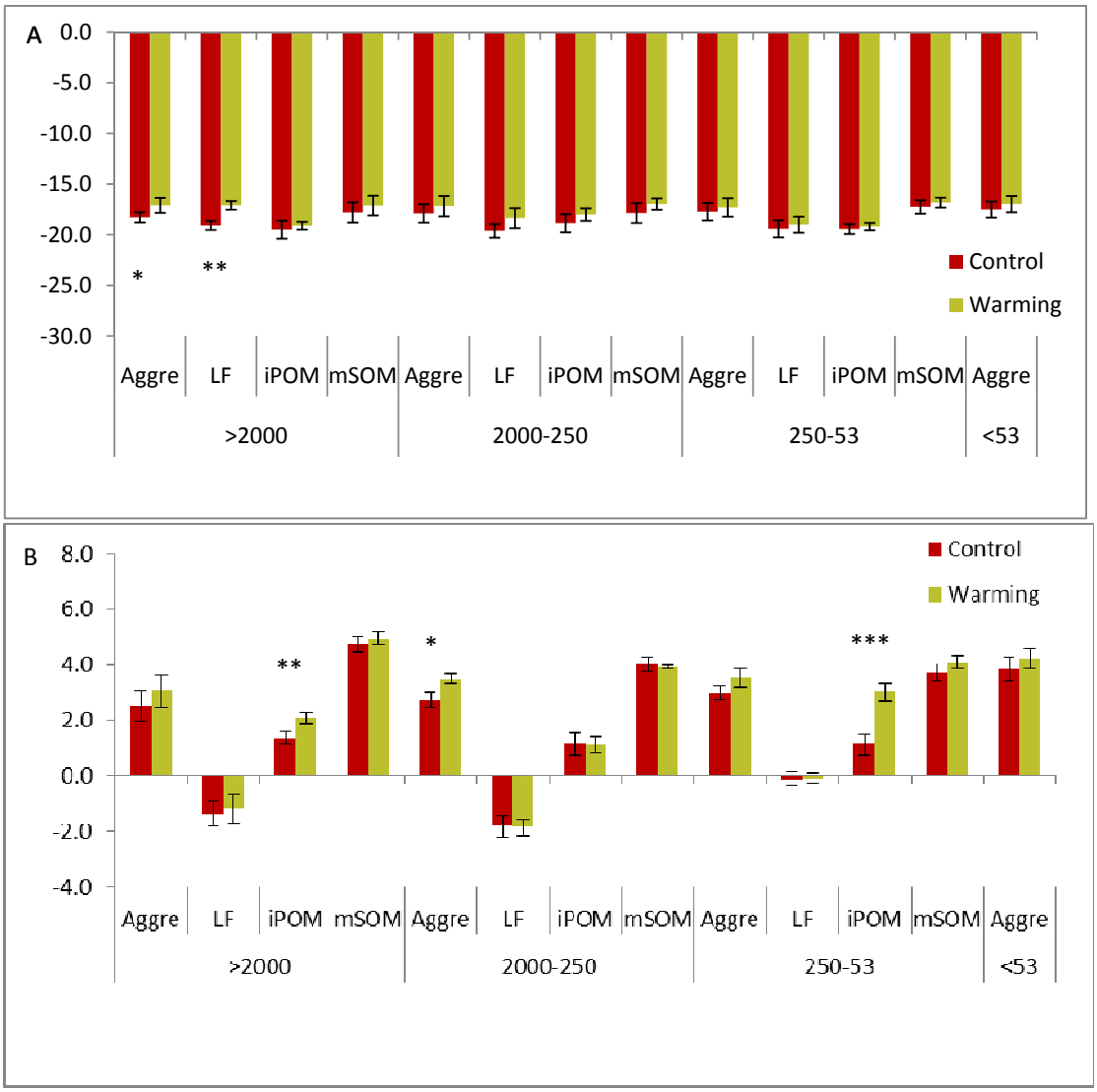

Fig. S7. The $\delta^{13}C$ **(A)** and $\delta^{15}N$ **(B)** values for soil light fraction (LF), intra-aggregate particulate organic matter (iPOM) and mineral soil organic matter (mSOM) of different aggregate (Aggre) sizes (μm) from control and warming plots in 2008. Error bars indicate standard error of the data (n=6). The differences between warming and the control were tested by two-tailed paired t-tests and labeled with *** when $p<0.01$, ** when $p < 0.05$, and * when $p < 0.10$.

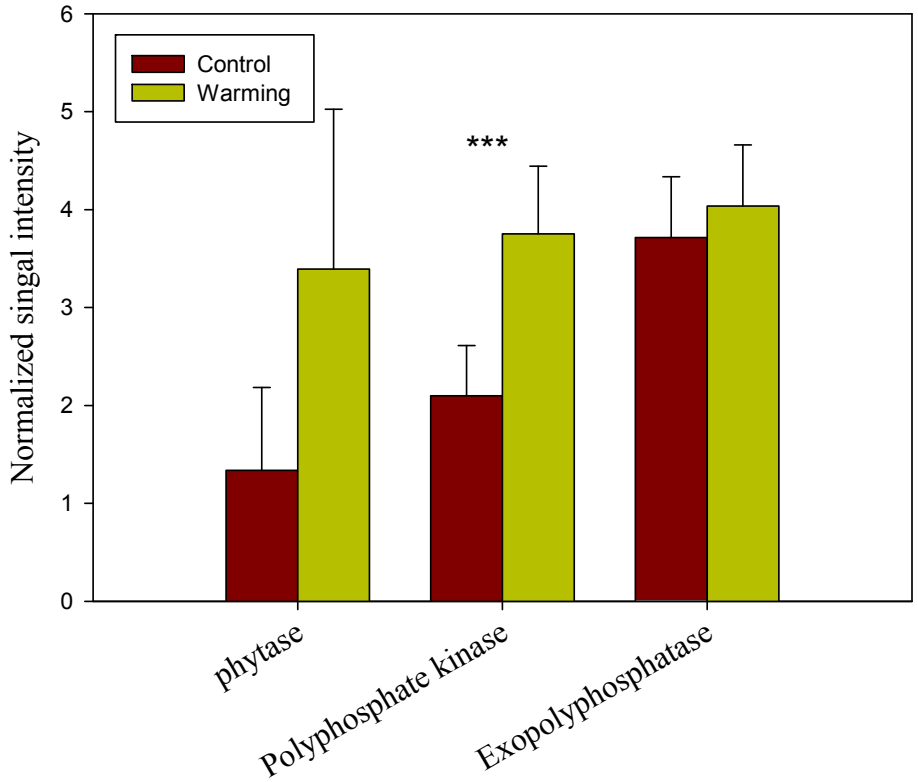

168

169 **Fig. S8.** The normalized average signal intensity of the detected phosphorus utilization genes under
170 warming and the control in 2007. Signal intensities were averaged and normalized by the probe
171 number for each gene. Error bars indicate standard error of the data (n=6). The differences between
172 warming and control were tested by two-tailed paired t-test and labeled with *** when $p < 0.01$.

173

SUPPLEMENTARY MATERIALS AND METHODS

1. Site Description and Sampling

This study was conducted at the Kessler Farm Field Laboratory (KFFL) located at the Great Plain Apiaries in McClain County, Oklahoma, USA (34°58'54"N, 97°31'14"W). This is an old field tall grass prairie that had been abandoned from agriculture for more than 30 years. The herbivores were excluded at this site in 2002 to prevent light grazing, which occurred before. The grassland is dominated by C_4 grasses (*Andropogon gerardii, Sorghastrum nutans, Schizachyrium scoparium, Panicum virgatum, and Eragrostis spp.*), C_3 forbs (*Ambrosia psilostachyia and Xanthocephalum texanum*), and C3 annual grass (*Bromus japonicas)*[1,2]. Based on Oklahoma Climatological Survey from 1948 to 1999, the mean annual temperature at this site was 16.3ºC with the lowest, 3.3ºC, in January and the highest, 28.1ºC, in July, while the mean annual precipitation was 967mm, which was highest in May and June (240 mm) and lowest in January and February (82 mm). The soil is silt loam (36% sand, 55% silt, and 10% clay in the top 15 cm) and part of Nash–Lucien complex, which typically has high fertility, neutral pH, high available water capacity, and a deep moderately penetrable root zone[3].

The experiment was established in November 1999 with a blocked split-plot design, in which warming is a primary factor. Two levels of warming (ambient and +2ºC) were set for six pair of 1 m ×1 m subplots by utilizing a "real" or "dummy" infrared radiator (Kalglo Electronics, Bethlehem, Pennsylvania) as the heating device, suspended 1.5m above the ground in warming plots. In control plots, the dummy infrared radiator is suspended to exclude a shading effect of the device itself on treatments.

2. Aboveground and Belowground Net Primary Production

Aboveground plant biomass (AGB) was indirectly estimated by pin-contact counts[4] each year. The pin frame is 0.5 m long and holds 10 pins 5 cm apart at 30° from vertical. Pins were 0.75 m long each and could be raised within the frame to count hits up to 1 m high (hits above 1 m are negligible at this site). In each subplot, the point frame was placed four times in each of the four cardinal directions to record the contact numbers of the pins separately with green and brown plant tissues (i.e., leaves and stems). The brown tissues were considered to be dead plant materials produced in the current year. The contact numbers of both green and brown tissues were then used to estimate AGB using calibration equations derived from 10 calibration plots, which were randomly selected each season and year and located at least 5 m away from the experimental plots. Biomass in the

calibration plots was clipped to the ground surface instead of 10 cm above the ground. Clipped plant materials were oven-dried and then correlated with the total contact number. A linear regression of total hits vs. total biomass was used to derive the calibration equation. The estimated AGB during the peak season in summer (July or August) was considered to be aboveground net primary production (ANPP) since our ecosystem satisfied primary criteria of virtually no carryover of living biomass from previous years due to a distinct dormant season and negligible decomposition of biomass produced during the growing season[5], but a conversion factor of 2.1 was applied as the measurement was only for above 10 cm biomass. Biomass was converted to C content by a factor of 0.45.

The root biomass was measured by taking soil cores (5.2 cm in diameter and 45 cm in depth) from one unclipped subplot. The roots were oven-dried at 65 °C for 48 h. The belowground net primary production (BNPP) was estimated from root biomass and root turnover rates. Root turnover was quantified in this area of our study[6,7] and correlated with temperature according to a meta-analysis of 62 studies in temperate grasslands[8]. From the temperature–turnover relationship, we estimated a root turnover rate using a mean annual temperature of 16.3 °C at our site. The estimated turnover rate is slightly higher but within a range of the measured ones in the literature[6,7]. Then, deviations of the 62 observed root turnover rates in the meta-analysis database were computed from the temperature–turnover regression line as an estimate of variance for the turnover rate.

3. Labile C and total organic C

A two-step acid hydrolysis procedure was adopted in this study to determine the labile and recalcitrant C pools in soils as described previously[9]. Briefly, a 500 mg soil sample was hydrolyzed with 20 ml of 5 N H_2SO_4 at 105ºC for 30 min. The hydrolysate and the 20 ml water washing to the residue were recovered by centrifugations and decantations as labile pool 1, predominantly containing polysaccharides. After drying at 60ºC, the remaining residue was added with 2 ml 26 N H_2SO_4 overnight at room temperature, under continuous shaking. The 24 ml water were added to dilute the acid to be 2N and hydrolyzed at 105 ºC for 3 h. The hydrolysate and the 20 ml water washing to the residue was taken as labile pool 2, largely containing cellulose.

The total organic C in soils and labile pool 1 and 2 were measured by a Shimadzu TOC-5000A Total Organic Carbon Analyzer with ASI-5000A Auto Sampler (Shimadzu Corporation, Kyoto, Japan) in the Stable Isotope/Soil Biology Laboratory at the University of Georgia (Athens GA). The recalcitrant C pools were calculated as the difference between soil TOC and organic C in labile pools

(1 and 2).

4. Soil Carbon, Nitrogen and Stable Isotope Analyses

Based on a developed protocol[10], the aggregate separation and size density fractionations were performed for air-dried soil samples collected from 0-20 cm depth by soil cores (4 cm in diameter) in the fall of 2008. The large roots and stone had been removed by hand from soils.

A series of sieves (2000, 250, and 53 μm) were used to separate four aggregate sizes. A 100 g dry soil was submerged with de-ionized water for 5 minutes at room temperature on the top of the 2000 μm sieve. Then the sieve with soil was manually shaken in vertical direction at a speed of 25 times min^{-1} for 2 min. The stable aggregates (> 2000 μm) were gently washed off into an aluminum pan. Floating organic materials (> 2000 μm) were discarded as they are not considered to be soil organic matter (SOM). These steps were repeated using the other two sieves (one at a time), but the floating material was retained. Finally four size fractions were obtained (>2000 μm, 250 - 2000 μm, 53 - 250 μm and <53 μm). The aggregates were oven dried at 50°C, weighed and stored at room temperature.

The density fractionation was performed using 1.85 g cm^{-3} sodium polytungstate (SPT) solution, following the published protocol[10]. A subsample (5 g) of each oven-dried aggregate was suspended in 35 mL SPT and slowly shaken by hand. The material remaining on the cap and sides of the centrifuge tube was washed into the suspension with 10 mL of SPT. After 20 min of vacuum (138kPa), the samples were centrifuged (1250 *g*) at 20 ^{o}C for 60 min. The floating material (light fraction-LF) was aspirated onto a 20 μm nylon filter, subjected to multiple washings with deionized water to remove SPT, and dried at 50°C. The heavy fraction (HF) was rinsed twice with 50 mL of deionized water and dispersed in 0.5% sodium hexametaphosphate by shaking for 18 h on a reciprocal shaker. The dispersed heavy fraction was then passed through a 53 μm sieve and the material remaining on the sieve, i.e. the intra-aggregate particulate organic matter (iPOM) was dried (50°C) and weighed.

Subsamples from all fractions and the whole soil samples were treated with 1N HCl for 24 hours at room temperature to remove soil inorganic C (carbonates). The C and N concentration and $\delta^{13}C$ and $\delta^{15}N$ of soil were determined at the University of Arkansas Stable Isotope Laboratory on a Finnigan Delta^{+} mass spectrometer (Finnigan MAT, Germany) coupled to a Carlo Erba elemental analyzer (NA1500 CHN Combustion Analyzer, Carlo Erba Strumentazione, Milan, Italy) via a

120 Finnigan Conflo II Interface. The C and N contents of each fraction was calculated on an area basis,
121 adjusting by soil depth and density.

122 The C and N isotope ratios of the soil fractions are expressed as:

123 $$\delta^h X = \left[\left(\frac{X^h}{X^l} \right)_{sample} \Big/ \left(\frac{X^h}{X^l} \right)_{s\tan dard} - 1 \right] \times 1000 \qquad (1)$$

124 where X is for either C or N, h is the heavier isotope, l is the lighter isotope. The C isotope ratios (^{13}C)
125 are expressed relative to Pee Dee Belemnite ($\delta^{13}C = 0.0‰$); the N stable isotope ratios (^{15}N) are
126 expressed relative to air ($\delta^{15}N = 0.0‰$). Standards (acetanilide and spinach) were analyzed after
127 every ten samples; analytical precision of the instrument was ±0.13 for $\delta^{13}C$ and ±0.21 for $\delta^{15}N$.

128 **5. Soil respiration measurement and Q_{10} estimation (Inversion analysis)**

129 **a. Soil respiration measurement**

130 Soil respiration was measured once or twice a month between 10:00 and 15:00 (local time) using a
131 LI-COR 6400 portable photosynthesis system attached to a soil CO_2 flux chamber (LI-COR Inc.,
132 Lincoln, NE, USA). Measurements were taken above a PVC collar (80 cm^2 in area and 5 cm in depth)
133 and a PVC tube (80 cm^2 in area and 70 cm in depth) in each plot. The PVC tubes cut off old plant
134 roots and prevented new root from growing inside the tubes. After 5 months, the CO_2 efflux
135 measured above the PVC tubes represented the heterotrophic respiration. And the CO_2 efflux
136 measured above the PVC collars represented the total soil respiration including heterotrophic and
137 autotrophic respiration. Aboveground parts of living plants were taken out of the PVC tubes and
138 collars every time before the measurement.

139 **b. Q_{10} estimation**

140 We used the inverse analysis method to estimate the Q_{10} values for *monthly* heterotrophic soil
141 respiration in control and warming plots. The inverse analysis is also called the data-assimilation
142 method, which is widely used to incorporate experimental observations with the model to estimate
143 key parameters of ecosystem processes[11,12]. The major advantage of this approach is that it allows us
144 to assess heterotrophic respiration from field soil respiration data. In this case, we used a Bayesian
145 paradigm to incorporate a *priori* probabilistic density functions (PDF) with above ground biomass
146 and heterotrophic soil respiration measurements from 2000 to 2007 to generate a *posteriori* PDF for
147 Q_{10} values for heterotrophic soil respiration. In this case, we estimated five parameters (heterotrophic
148 soil respiration Q_{10}, autotrophic soil respiration Q_{10}, microbial biomass carbon residence time, fine

litter biomass residence time, and root biomass residence time) using four data sets (heterotrophic soil respiration, autotrophic soil respiration, aboveground biomass, and belowground biomass) in a revised terrestrial ecosystem (TECO) model[13], which is a process-based model developed to examine critical ecosystem processes regarding plant responses to climate changes. The TECO model has four major components: canopy photosynthesis sub-model, soil water dynamic sub-model, plant growth (allocation) sub-model, and soil C transfer sub-model. The model was calibrated for the warming experiments in Kessler Farm Field Laboratory. The result is a constructed marginal distribution of the PDFs. The peak of each line represents the Q_{10} with the highest possibility in that treatment, thus it also represents the best estimation of Q_{10}, and it will generate least error between the model simulated soil respiration and the soil respiration data.

To apply Bayes' theorem, we specified the prior PDFs $p(c)$ of parameters as a uniform distribution. The interval for Q_{10} values are between 2 and 5. The lower and higher limits were chosen based on previous studies of Q_{10} values on the same site using regression methods[14,15] as our prior knowledge of the parameter. Then we constructed the likelihood function $p(Z|c)$ based on the observation errors across all observation times. The fewer errors there are between the modeled results and observations are, the higher the likelihood of the parameter. At last, with Bayes' theorem, the posterior PDF $p(c|Z)$ is given by

$$p(c|Z) \propto p(Z|c)\, p(c).$$

The parameters were sampled by the Metropolis-Hastings (M-H) Algorithm[16,17]. The M-H algorithm is a Markov Chain Monte Carlo (MCMC) technique to reveal the PDF of the parameter via a sampling procedure. In short, to generate Markov Chain, the two steps in M-H algorithm, a proposing step and a moving step, were run repeatedly. Each proposing step generates a new set of parameters based on the previously accepted set of parameters, and then in the moving step the newly generated parameters are tested against the Metropolis criterion to decide whether it should be accepted. In our case, we ran the TECO model with each proposed parameter, and then we compared modeled data (soil respiration and biomass) with the data observed in the field. If newly proposed parameters produce less error between the modeled and observed data than previous parameters, they will always be accepted. If they are worse than the previous parameters, they will be accepted at a possibility that is dependent on the relative performance of the old and the new parameters. If newly proposed parameters are rejected, a new set of parameters will be proposed from the parameters that are accepted in the previous step. The sampling began with a randomly selected starting point from the prior PDF, and then 50,000 sampling procedures were performed for each treatment: control or warming. The first 1,000 accepted parameter sets were discarded, and the remaining accepted

parameter sets were used for each treatment.

We constructed the *a posteriori* PDF of heterotrophic Q_{10} based on the posterior distribution of Q_{10} obtained in the previous steps. The maximum likelihood estimates were identified by observing the parameter values corresponding to the peaks of their PDF.

6. Laboratory Incubation for N processes

Soil sample were collected by soil cores (4 cm in diameter and 20 cm in depth) from the field in Oct 3, 2010. Laboratory incubations were conducted to measure the denitrification potential. Soil samples (20 g, oven dry weight equivalent) were placed into 74 ml bottles, 9 mg $K^{15}NO_3$-N (98 atom % ^{15}N, Sigma-Aldrich, St. Louis, MO, USA) was added, and adjusted to 70% water holding capacity. After evacuation, the headspace of each bottle was filled by unlabeled N_2 (Airgas Inc., Radnor, PA, USA). At 1, 3 and 6 days after the initiation of incubation at room temperature, a 12 ml gas sample from the headspace of each bottle was collected into evacuated Exetainers with plastic screw-caps (Labco Ltd, High Wycombe, UK). After each sampling time point, the bottles were evacuated and filled by unlabeled N_2 again. The gas samples were sent to the Stable Isotope Facility at the University of California, Davis (Davis, CA) to determine the concentration of $^{15}N_2$ and $^{15}N_2O$ by the ThermoFinnigan GasBench + PreCon trace gas concentration system interfaced to a ThermoScientific Delta V Plus isotope-ratio mass spectrometer (Bremen, Germany). The denitrification potential was represented by the $^{15}N_2O$ and $^{15}N_2$ products generated during the incubation.

7. Soil sampling for molecular analyses

Twelve soil samples were taken from the 0-15 cm layer of 6 warming and 6 control plots both in April 2007 and October 2008. Each sample was composited from four soil cores (2.5 cm diameter × 15 cm deep) after being sieved by 2mm sieves to have enough samples for soil chemistry, microbiology and molecular biology analyses. All samples were transported to the laboratory immediately and stored at -80^{o}C.

To determine whether long-term warming affects microbial community structure, several metagenomic and conventional microbial analyses were performed, including (i) Phospholipid fatty acid (PLFA) analysis[19] for 2008 samples, which provides information on the physiological activity of microbial communities[20]; (ii) Enzyme activity[21,22] for 2008 samples; (iii) BIOLOG analysis to examine substrate utilization profile patterns; (iv) Labile C and total soil organic C analyses[9] for 2008 samples; (v) Functional gene array (i.e., GeoChip 3.0)[23] for 2007 samples, which measure the functional structure of microbial communities; and (vi) 16S rRNA gene-based targeted pyrosequencing[24] for 2007 samples, which assesses the phylogenetic composition of microbial communities. Since the microbial communities in the experimental site has been warmed for more

than 8 years, DNA-based microbial population abundance changes should be more appropriate to reflect microbial activity changes than mRNA-based analysis due to their very short half life (~ 3 min). Thus, in this study, we rely on DNA-based analysis to measure population changes.

a. Phospholipid fatty acids (PLFA)

Microbial biomass was estimated by PLFA analysis. The PLFAs were extracted from 3.0 g soil by a modified[25] technique as previously described[19] and analyzed by a Hewlett-Packard Agilent 6890A gas chromatograph (GC) (Agilent Tech. Co., USA) equipped with an Agilent Ultra-2 (5% phenyl)-methylpolysiloxane capillary column (25 m by 0.2 mm by 0.33 mm) and flame ionization detector (FID). All PLFAs were used for estimating total microbial biomass.

The PLFAs selected to represent bacteria biomass included a15:0, i15:0, 15:0, a17:0, cy17:0, i17:0, 17:0, 16:1ω5c, 16:1ω9c, 18:1ω5c, while the fungal biomass was calculated only based on 18:1ω9c[4,26,27]. The detected PLFAs were notablly low in sample 2UW and too many missing values occurred for PLFAs that are commonly observed in other soils samples. In this way, 2UW was excluded from any further data analysis related to PLFAs.

b. Enzyme activity

Extracellular enzyme activities of phenol oxidase and peroxidase involved in lignin decomposition were analyzed as described previously[21,22] with modifications. Both enzymes were assayed spectrophotometrically using 3, 4-dihydroxy-L-phenylalanine (L-DOPA) as the substrate, followed by quantification of a red oxidation product of L-DOPA. The activities were standardized using a commercial L-DOPA oxidase, mushroom tyrosinase (Sigma T3824). Briefly, a soil suspension was prepared by adding 1 g of soil to 125 mL modified universal buffer (MUB) (50 mM, pH 5.5) in a 300-mL Pyrex tall-form beaker and then mixed with a magnetic stir bar for 30 min for complete homogenization. Following settling for 30 min, 150 μL of suspension was dispensed into each well of a 96-well microplate using a 0-250 μL multi-channel pipette with wide orifice tips. For phenol oxidase assays, 50 μL of 10 mM L-DOPA was added to each microplate well as the substrate. For peroxidase assays, 50 μL of 10 mM L-DOPA plus 10 μL of 0.3% H_2O_2 were added to each microplate well. The reactions were mixed by pipetting up and down several times before incubating in the dark at 25ºC for 18 hours. Triplicate analyses were performed for each sample and its control, for which the substrate solution was added upon completion of the incubation. The enzyme activities were quantified by measuring absorbance at 450 nm using a Benchmark microplate reader with an auto-mixing feature (Bio-Rad Laboratories, Hercules, CA, USA) based on the following formula:

Phenoloxidase (mM) = $Abs_{450}/\varepsilon l$

Peroxidase (mM) = $Abs_{450}/\varepsilon l$-*phenoloxidase activity*

where ε is the extinction coefficient, which is 1.79 mM^{-1} cm^{-1} for L-DOPA under the conditions of this assay and l is the wavelength path, which is 0.52 cm.

The ε value was determined by adding a known quantity of mushroom tyrosinase to completely oxidize a known amount of L-DOPA and then measuring the absorbance of the reaction product. Briefly, 50 μL of a 10 mM solution of L-DOPA was incubated in the dark at 25°C with 150 μL of 1 mg mL^{-1} mushroom tyrosinase solution for at least 6 h (indicated by maximum absorbance at 450 nm). Subsequently, absorbance of the solution was measured. The extinction coefficient was calculated according to Beer's law with the assumption of quantitative oxidation of L-DOPA to quinine under the assay conditions. The wavelength path for 200 μL of reaction mixture in the microplate well used was 0.52 cm. The ε value was calculated using the equation described below:

$\varepsilon = Abs_{450}$ / [substrate volume (50 μL) x substrate concentration (10 mM) / total volume (200 μL)] / wavelength path (0.52 cm)

c. BIOLOG analysis

The substrate utilization patterns of soil microbial communities was analyzed by ECO MICROPLATE™ (BIOLOG, CA, USA). Soil (5 g) was put into a 50 ml centrifuge tube and 50 ml sterile deionized water was added. The mixture of soil and water was shaken at 200 rpm for 45 min and allowed to settle for 30 min at 4°C. Then the mixture was serially diluted (10^{-1}, 10^{-2}, 10^{-3}), and the 10^{-3} dilution was loaded into the wells of the ECO MICROPLATE. The plates were incubated in a Biolog OmniLog PM System at 25°C for 48 hours. The color change of each well was captured by the moving camera and the average well color development (AWCD) was calculated by averaging the optical densities (OD) in all wells containing various C sources and normalized by the detection in control wells.

d. DNA extraction

Soil DNA was extracted by freeze-grinding mechanical lysis as described previously[28] and was purified using a low melting agarose gel followed by phenol extraction for 12 soil samples collected in 2007. DNA quality was assessed based on the ratios of 260 /280 nm and 260/230 nm absorbance by a NanoDrop ND-1000 Spectrophotometer (NanoDrop Technologies Inc., Wilmington, DE), while final soil DNA concentrations were quantified by PicoGreen[29] using a FLUOstar Optima (BMG Labtech, Jena, Germany).

8. GeoChip analysis

GeoChip 3.0 was used for this study for 12 samples taken in 2007. The GeoChip 3.0 contains approximately 28,000 probes and covers about 57,000 gene sequences in more than 292 gene

families[30]. GeoChip analyses were performed as described previously[31,32] with the following steps:

a. Template amplification

In order to produce consistent hybridizations from all samples, a whole community genome amplification (WCGA)[32] was used to generate approximately 2.5-4.0 μg of DNA with 50 ng purified DNA as the template using the TempliPhi Kit (GE Healthcare, Piscataway, NJ) following the manufacturer's instructions. In addition, single-strand binding protein (267 ng μL^{-1}) and spermidine (0.1 mM) were added to the reaction mix to improve the amplification efficiency and representation. The reactions were incubated at 30°C for 3 hours and stopped by heating the mixtures at 65°C for 10 min.

b. Template labeling

After amplification, 2.5 μg DNAs were labeled with the fluorescent dye Cy-5 using random priming as follows. First, the amplified DNAs were mixed with 20 μL random primers, denatured at 99.9°C for 5 min, and then immediately chilled on ice. Following denaturation, the labeling master mix containing 2.5 μL dNTP (5 mM dAGC-TP, 2.5 mM dTTP), 1 μL Cy-5 dUTP (Amersham, Piscataway, NJ), 80 U of the large Klenow fragment (Invitrogen, Carlsbad, CA), and 2.5 μL water were added and then incubated at 37°C for 3 hours, followed by heating at 95°C for 3 min. Labeled DNA was purified using the QIA quick purification kit (Qiagen, Valencia, CA) according to the manufacturer's instructions, measured on a NanoDrop ND-1000 spectrophotometer (NanoDrop Technologies Inc., Wilmington, DE), and then dried down in a SpeedVac (ThermoSavant, Milford, MA) at 45°C for 45 min.

c. Hybridization and imaging processing

The labeled target DNA was resuspended in 120 μl hybridization solution containing 50% formamide, 3 x SSC, 10 μg of unlabeled herring sperm DNA (Promega, Madison, WI), and 0.1% SDS, and the mix was denatured at 95°C for 5 min and kept at 50°C until it was deposited directly onto a microarray. Hybridizations were performed with a TECAN Hybridization Station HS4800 Pro (TECAN, US) according to the manufacturer's protocol. After washing and drying, the microarray was scanned by ScanArray Express Microarray Scanner (Perkin Elmer, Boston, MA) at 633 nm using a laser power of 90% and a photomultiplier tube (PMT) gain of 75%. The ImaGene version 6.0 (Biodiscovery, El Segundo, CA) was then used to determine the intensity of each spot, and identify poor-quality spots. A total of 5537 functional genes were detected by GeoChip hybridization.

d. Data pre-processing

Raw data from ImaGene were submitted to Microarray Data Manager on our website (http://ieg.ou.edu/microarray/) and analyzed using the data analysis pipeline with the following major steps: (i) The spots flagged as 1 or 3 by ImaGene and with a signal to noise ratio (SNR) less

than 2.0[33] were removed as poor-quality spots; (ii) After removing the bad spots, the normalization was performed at three levels: individual sub-grids on a single slide, technical replicates among samples and across the whole data set. First, the mean Cy3 intensity of the universal standards in each sub-grid was used to normalize the Cy5 intensity for probes in the same sub-grid. Second, the Cy5 intensity after the first normalization was normalized again by the mean value of three technical replicates. In addition, the data was normalized by the mean intensity of universal standards (Cy3 channel) in all slides for Cy5 intensity of samples; (iii) If any replicates had (signal–mean) more than two times the standard deviation, this replicate was removed as an outlier. This process continued until no such replicates were identified; (iv) At least 0.34 time of the final positive spots (probes), or a minimum of two spots was required for each gene to be considered for data analysis; and (v) If a probe appeared in only one sample among the total of six for warming or control, it was removed for all further analyses. After that, the relative abundance in each sample was calculated by dividing the individual signal intensity of each probe by the sum of original signal intensity for all detected probes in that sample. Then the relative abundance was multiplied by the mean value for the sums of original signal intensity in all samples. A natural logarithm transformation was performed for the amplified relative abundance plus 1. Altogether, a total of 2357 functional genes were detected.

9. 454 pyrosequencing analysis

a. Sample tagging and PCR amplicon preparation

Based on the V4-V5 hypervariable regions of bacterial 16S rRNA (*Escherichia coli* positions 515-907), the PCR primers, F515: GTGCCAGCMGCCGCGG, and R907: CCGTCAATTCMTTTRAGTTT were selected. Both primers were then checked with the ribosomal database[34], and covered > 98% of the 16S gene sequences in the database (July 2007). To pool multiple samples for one run of 454 sequencing, a sample tagging approach was used[35,36]. In this study, 2-3 unique 6-mer tags were used for each of 12 DNA samples. Each tag was added to the 5'-end of both forward and reverse primers, and those tag-primers were synthesized by Invitrogen (Carlsbad, CA) and used for the generation of PCR amplicons. The amplification mix contained 10 units of Pfu polymerase (BioVision, Mountain View, CA), 5 µl Pfu reaction buffer, 200 µM dNTPs (Amersham, Piscataway, NJ), and a 0.2 µM concentration of each primer in a volume of 50 µl. Genomic DNA (10 ng) was added to each amplification mix. Cycling conditions were an initial denaturation at 94°C for 3 min, 30 cycles of 95°C 30 s, 58°C for 60 s, and 72°C for 60 s, a final 2-min extension at 72°C. Normally, multiple (5-10) 50-µl reactions were needed for each sample, and the products were pooled together after amplification and purified by agarose gel electrophoresis. The amplified PCR products were recovered and then quantitated with PicoGreen[29] using a FLUOstar Optima (BMG Labtech, Jena, Germany). Finally, amplicons of all samples were pooled in

an equimolar concentration for 454 pyro-sequencing. Each sample was labeled with multiple (two or three) but unique tags.

b. 454 pyrosequencing

The fragments in the amplicon libraries were repaired and ligated to the 454 sequencing adapters, and resulting products were bound to beads under conditions that favor one fragment per bead. The beads were emulsified in a PCR mixture in oil, and PCR amplification occurred in each droplet, generating millions of copies of a unique DNA template. After breaking the emulsion, the DNA strands were denatured, and beads carrying single-stranded DNA clones were deposited into wells on a PicoTiter-Plate (454 Life Sciences) for pyrosequencing[37] on a FLX 454 system (454 Life Sciences, Branford, CT). For this study, we recovered both forward and reverse reads of 12 samples with an average length around 240 bp. All pyrosequencing reads were initially processed using the RDP pyrosequencing pipeline (http://pyro.cme.msu.edu/pyro/index.jsp)[34].

c. Removal of low-quality sequences

To minimize effects of random sequencing errors, we eliminated (*i*) sequences that did not perfectly match the PCR primer at the beginning of a read, (*ii*) sequences with non-assigned tags, (*iii*) sequence reads with < 200 bp after the proximal PCR primer if they terminated before reaching the distal primer, and (*iv*) sequences that contained more than one undetermined nucleotide (N). Only the first 240 bp after the proximal PCR primer of each sequence was included since the quality of sequences degrades beyond this point.

d. Assignment of sequence reads to samples

The raw sequences were sorted and distinguished by unique sample tags and each sample had 2 or 3 unique tags as replicates. The tag and primers were then trimmed for each replicate. There were 15 replicate datasets for each treatment, warming or control. For all 30 replicates, the number of sequence reads ranged from 1033 to 5498. A total of 65,736 effective sequences were obtained.

e. Classification of 454 sequences and assignment of phylotype OTUs

All sequences of the 12 samples were aligned by RDP Infernal Aligner that was a fast secondary-structure aware aligner[38] and then a complete linkage clustering method was used to define OTUs within a 0.03 difference[39]. The singleton OTUs (with only one read) were removed, and the remained sequences (S) were sorted into each sample based on OTU. The relative abundance (RA) was calculated as following equation:

$$RA_{ij} = \frac{S_{ij}}{\sum_{j=1}^{N} S_{ij}}$$

where *i* is the i^{th} sample (1 to m), and *j* is the j^{th} OTU (1 to n). The sequences of OTUs were then assigned to a taxonomy by the RDP classifier[40] with a confidence cutoff of 0.8. The lineage of each OTU was summarized with all phylogenetic information.

If an OTU only appeared in three or fewer samples among the total 15 datasets for each treatment, it was removed, resulting in 2561 OTUs used further analysis. The number of detected OTUs at different levels of classification was counted for warming or control. Then the average of OTUs among replicated tags for each plot was used for statistical analysis.

10. Statistical analysis

The matrices of microarray data resulting from our pipeline were considered as 'species' abundance in statistical analyses. For pyrosequencing data, the relative percentage of each OTU, or the sum of OTUs at a specific taxonomic (phylum, class, order, or family) level was used as the relative abundance of OTU, family, order, class, or phylum. The microbial diversity indices were analyzed by R software version 2.9.1 (The R foundation for Statistical Computing).

Detrended correspondence analysis (DCA) was employed to determine the overall functional changes in the microbial communities by R software version 2.9.1 as well. DCA is an ordination technique that uses detrending to remove the arch effect, where the data points are organized in a horseshoe-like shape, in correspondence analysis[41].

Different datasets of microbial communities generated by different analytical methods were used to examine whether elevated temperature has significant effects on soil microbial communities. Typically, it is difficult for all datasets to meet the assumptions (e.g. normality, equal variances, independence) of parametric statistics. Thus, in this study, three different complementary non-parametric analyses for multivariate data were used: analysis of similarity (ANOSIM)[42], non-parametric multivariate analysis of variance (adonis) using distance matrices[43], and multi-response permutation procedure (MRPP). We used the Bray-Curtis similarity index to calculate a distance matrix from GeoChip hybridization data for ANOSIM, adonis and MRPP analyses. MRPP is a nonparametric procedure that does not depend on assumptions such as normally distributed data or homogeneous variances, but rather depends on the internal variability of the data[44,45]. All three methods are based on dissimilarities among samples and their rank order in different ways to calculate test statistics, and the Monte Carlo permutation is used to test the significance of statistics. All three procedures (anosim, adonis and mrpp) were performed with the Vegan package (v.1.15-1) in R software version 2.9.1 (The R foundation for Statistical Computing).

Canonical correspondence analysis (CCA) was performed to determine the most significant plant and soil variables shaping microbial community composition and structure[31,46,47]. For constructing the CCA model, the maximum number of constrained variables used must be less than the number of

samples (m), i.e., m-1. Since the measured plant and soil variables (37 variables) were more than the number of samples (12 samples), several approaches were used to select the most significant variables. One is to use the Mantel test to examine the correlation between community structure and each variable. Only significant variables by the Mantel test ($p<0.1$) (8 variables) were considered for further analysis. Using automatic forward selection in CCA, 11 variables were selected. Then the 16 selected plant and soil variables from the Mantel test and CCA were combined. However, some important variables in terms of biology were still missing. The soil pH value, which was not selected by these two methods, was also included for constructing CCA models. According to the variance inflation factors (VIF) values, some redundant variables (VIF>20) have been removed from the CCA model. Finally, a total of 9 environmental factors were selected, including leaf area index (LAI), belowground net primary productivity (BNPP), aboveground net primary productivity (ANPP), C_4 aboveground net primary productivity (C_4-ANPP), soil temperature (Tm), moisture (MS), pH, total organic C (TOC) and N (TON). All CCA and partial CCA were performed by the vegan package in R[48,] except the forward selection from Conoco software[49].

To test the significance of the differences between warming and control treatment for various variables, two-tailed paired t tests was employed by Microsoft Excel 2010 (Microsoft Inc., Seattle, WA). For gene abundances, we did not adjust p-values of statistic tests using the Bonferroni procedure due to its overly conservative nature as following Moran's opinions[50,51].

One-tailed paired tests were also performed to improve the power of the t-test[52] for certain ecosystem parameters which are expected to increase or decrease under warming based on our previous knowledge. These parameters were: belowground net primary productivity, litter input to soil, bacterial and fungal gene abundance detected by GeoChip, soil NH_4 content, soil N availability, and $\delta^{15}N$. One tailed paired t-tests appeared to be appropriate for these variables because the directions of change for these parameters can be predicted based on our previous knowledge. Our plant biomass data demonstrated that above ground biomass increased significantly and plant species composition has shifted toward C4 dominance. Thus, it is expected that the belowground net primary productivity and litter input to soil increase rather than decrease under warming. Second, due to more C input to soil, an increase of soil microbial biomass is expected, reflected by detected gene abundances of bacteria and fungi. Third, increases in plant biomass under warming could increase N uptake by plants, which could lead to lower soil NH_4 content and N availability under warming. In addition, the genes involved in N cycling, including denitrification, were significantly higher under warming, it is anticipated that $\delta^{15}N$ decreases due to the possibly accelerating N process rates and more N product from microbially mediated processes escaping from the soil system, like N_2O and N_2 from denitrification.

The one-tailed statistical test is often used in ecology, animal behavior and social sciences[53]. It has an advantage of increasing the power of a test[52]. Although using a one-tailed t-test potentially increases Type I errors (the rejection of a true null hypothesis), it could potentially lead to a decrease Type II error (acceptance of a false null hypothesis). In most practical applications, one goal is to keep both of these errors small because a null hypothesis should be not rejected when it is true or it should not be accepted when it is wrong. Although a one tailed test is not preferred, we believe that it still has merit if it is carefully used and the results are appropriately interpreted.

D. SUPPLEMENTARY REFERENCES

1. R. A. Sherry *et al.*, *Global Change Biol.* **14**, 2923 (2008).
2. W. J. Zhang, W. Zhu, S. Hu, *J. Environ. Sci.* **17**, 705 (2005).
3. USDA, Soil Survery of McClain Country, Oklahoma, Agricultural Experimental Station, Stillwater (1963).
4. D. A. Frank, S. J. Mcnaughton, *Oikos* **57**, 57 (1990).
5. A. K. Knapp, J. M. Briggs, D. L. Childers, O. E. Sala, in *Principles and Standards for Measuring Primary Production,* T. Fahey, A. Knapp, Eds. (Oxford University Press, Oxford, 2007), pp. 27-48.
6. J. Marshall, in *The Belowground Ecosystem: A Synthesis of Plant-Associated Process,* J. Marshall, Ed. (Colorado State University, Fort Collins, CO, 1977), pp. 73-84.
7. P. Sims, J. Singh, *J. Ecol.* **66**, 573 (1978).
8. R. A. Gill, R. B. Jackson, *New Phytol.* **147**, 13 (2000).
9. A. Belay-Tedla, X. H. Zhou, B. Su, S. Q. Wan, Y. Q. Luo, *Soil Biol. Biochem.* **41**, 110 (2009).
10. J. Six, E. T. Elliott, K. Paustian, J. W. Doran, *Soil Sci. Soc. Am. J.* **62**, 1367 (1998).
11. B. H. Braswell, W. J. Sacks, E. Linder, D. S. Schimel, *Global Change Biol.* **11**, 335 (2005).
12. W. Knorr, J. Kattge, *Global Change Biol.* **11**, 1333 (2005).
13. E. S. Weng, Y. Q. Luo, *J. Geophys Res.Biogeo.* **113**, (2008).
14. Y. Q. Luo, S. Q. Wan, D. F. Hui, L. L. Wallace, *Nature* **413**, 622 (2001).
15. X. Zhou, S. Q. Wan, Y. Q. Luo, *Global Change Biol.* **13**, 761 (2007).
16. W. K. Hastings, *Biometrika* **57**, 97 (1970).
17. N. Metropolis, A. W. Rosenbluth, M. N. Rosenbluth, A. H. Teller, E. Teller, *J. Chem. Phys.* **21**, 1087 (1953).
18. D. H. Buckley, V. Huangyutitham, S. F. Hsu, T. A. Nelson, *Appl. Environ. Microb.* **73**, 3196 (2007).
19. T. C. Balser, M. K. Firestone, *Biogeochem.* **73**, 395 (2005).
20. H. G. Chung, D. R. Zak, P. B. Reich, D. S. Ellsworth, *Global Change Biol.* **13**, 980 (2007).
21. B. Hendel, R. L. Sinsabaugh, J. Marxsen, in *Methods to Study Litter Decomposition: A Practical Guide. ,* F. Bärlocher, M. A. S. Graça, M. O. Gessner, Eds. (Springer, Netherlands, 2005), pp. 273-278.
22. K. R. Saiya-Cork, R. L. Sinsabaugh, D. R. Zak, *Soil Biol. Biochem.* **34**, 1309 (2002).
23. Z. L. He *et al.*, *Isme J.* **1**, 67 (2007).
24. M. L. Sogin *et al.*, *Proc. Natl. Acad. Sci. U.S.A.* **103**, 12115 (2006).

25. E. G. Bligh, W. J. Dyer, *Can. J. Biochem. Phys.* **37**, 911 (1959).
26. E. Baath, A. Frostegard, H. Fritze, *Appl Environ Microb* **58**, 4026 (1992).
27. J. R. Vestal, D. C. White, *Bioscience* **39**, 535 (1989).
28. J. Z. Zhou, M. A. Bruns, J. M. Tiedje, *Appl. Environ. Microb.* **62**, 316 (1996).
29. S. J. Ahn, J. Costa, J. R. Emanuel, *Nucleic Acids Res.* **24**, 2623 (1996).
30. Z. L. He *et al.*, *Isme J.* **4**, 1167 (2010).
31. Z. L. He *et al.*, *Ecol. Lett.* **13**, 564 (2010).
32. L. Y. Wu, X. Liu, C. W. Schadt, J. Z. Zhou, *Appl. Environ. Microb.* **72**, 4931 (2006).
33. Z. L. He, J. Z. Zhou, *Appl. Environ. Microb.* **74**, 2957 (2008).
34. J. R. Cole *et al.*, *Nucleic Acids Res.* **37**, D141 (2009).
35. J. Binladen *et al.*, *Plos One* **2**, (2007).
36. M. Hamady, J. J. Walker, J. K. Harris, N. J. Gold, R. Knight, *Nat. Methods* **5**, 235 (2008).
37. M. Margulies *et al.*, *Nature* **437**, 376 (2005).
38. E. P. Nawrocki, S. R. Eddy, *Plos Comput Biol.* **3**, 540 (2007).
39. E. Stackebrandt, B. M. Goebel, *Int. J. Syst. Bacteriol.* **44**, 846 (1994).
40. Q. Wang, G. M. Garrity, J. M. Tiedje, J. R. Cole, *Appl. Environ. Microb.* **73**, 5261 (2007).
41. M. O. Hill, H. G. Gauch, *Vegetatio* **42**, 47 (1980).
42. K. R. Clarke, *Aust. J. Ecol.* **18**, 117 (1993).
43. M. J. Anderson, *Aust. Ecol.* **26**, 32 (2001).
44. B. McCune, J. B. Grace, D. L. Urban, *Analysis of ecological communities*. (MjM Software Design, Gleneden Beach, OR, 2002), pp. iv, 300 p.
45. P. W. Mielke, K. J. Berry, *Permutation Methods: A Distance Function Approach*. (Springer, 2001).
46. A. Ramette, J. M. Tiedje, *Proc. Natl. Acad. Sci. U.S.A.* **104**, 2761 (Feb 20, 2007).
47. J. Zhou, S. Kang, C. W. Schadt, C. T. Garten, Jr., *Proc. Natl. Acad. Sci. U.S.A.* **105**, 7768 (2008).
48. P. Dixon, *J. Veg. Sci.* **14**, 927 (2003).
49. C. J. F. Terbraak, *Vegetatio* **75**, 159 (1988).
50. M.D. Moran, *Oikos* 100,403-405 (2003).
51. L. Jiang and S. N. Patel, *Ecology* 89: 1931-1940 (2008).
52. R. R. Sokal and F. J. Rohlf, *Biometry*, 3rd edn. Freeman, San Francisco (1995).
53. C.M. Lombardi and S.H. Hurlbert., *Austral Ecol* **34:** 447-468 (2009).

SUPPLEMENTARY TEXT

1. Microbial functional gene diversity

Our metagenomic and conventional microbial analyses suggested that long-term experimental warming dramatically altered the composition and structure of microbial communities. A total of 2,357 functional genes were detected by GeoChip hybridization, and 1,136 (48.2%) genes were overlapped between warming and control treatments. No significant differences were observed for the functional gene number and the diversity, as measured by Simpson Reciprocal index (1/D), between the warming and control samples (Table S2). Pyrosequencing recovered 2,561 OTUs (operational taxonomic units) with 1,200 (47%) OTUs overlapped between the warming and control plots. The detected number of OTUs and diversity were also not significantly different between warming and control samples (Table S2).

However, detrended correspondence analysis (DCA) showed that the samples from warming plots were clustered together and well separated from control plots based on both GeoChip (Fig. S1) and pyrosequencing (Fig. S2) data, suggesting that the microbial community composition and structure were markedly different between warming treatment and the control. To examine if those observed differences are statistically significant, three complimentary non-parametric multivariate statistical tests (ANOISM, adonis, and MRPP) were performed. The functional community structure revealed by GeoChip was significantly different between the warming and control plots with all three methods (Table 1). The phylogenetic community structure based on the 16S rRNA gene was also significantly different with at least one of the three methods (Table 1). Altogether, these results indicated that the composition, structure and potential functional activity of the microbial communities under experimental warming were significantly different from those in the control.

2. Linking microbial community composition and structure to aboveground and belowground processes

A total of 27 plant and soil variables were measured in this study. Based on forward selection and variance inflation factors (VIF < 15) with 999 Monte Carlo permutations, as well as Mantel test and biology, the following 9 variables were selected for linking microbial community composition and structure to aboveground and belowground processes: the average soil temperature, moisture (MS) and pH, total soil organic C, total soil N (TN), aboveground net primary production (ANPP), C_4 aboveground net primary production (C_4 ANPP), belowground net primary production (BNPP), and leaf area index (LAI). Statistical analysis showed that microbial community functional composition

and structure were significantly (F = 1.19, p = 0.025) shaped by these selected key plant and soil physical and chemical variables (Fig. S3A). Most significant variables were soil temperature (F=1.89, p = 0.001); soil pH (F=1.38, p=0.056), C_4 ANPP (F=1.68, p=0.008) and BNPP (F=1.58, p=0.034).

The relationships between microbial community structure and plant and soil variables are shown as a Biplot (Fig. S3A). The first two axes explained 35.7% of the constrained variations of the microbial community structure in which the first axis explained 21.5% of the variation while the second axis explained 14.2%. The samples from warming plots were most positively correlated with soil temperature, C_4 aboveground net primary production, belowground net primary production, total soil organic C and N whereas the samples from the control plots showed the opposite. These results suggested that temperature, C_4 aboveground net primary production, and belowground net primary production had most significant impacts on microbial community composition and structure.

To better understand how much each environmental variable influences the functional community structure, variation partitioning analysis (VPA)[1] was performed. The same variables used for CCA were used for VPA (Fig. S3B). A total of 32.0% variations of microbial communities can be explained by plant variables while soil variables can explain about 25.7% of the variations in community structure. In contrast to many other studies[1-3], considerably smaller portion (16%) of the community variations could not be explained by the selected plant and soil variables. These results implied that soil microbial community composition and structure at this site were primarily shaped by deterministic factors of plants and soils.

3. Substrate depletion vs acclimation

One of the greatest challenges in projecting future scenarios of climate warming is the uncertainty of the sensitivity of microbially mediated soil C decomposition to climate warming[4-6]. Whether the decline in the response of soil respiration to warming is due to microbial adaptation or substrate depletion is under intensive study and debate[4,5,7-9]. Most global climate models that couple climate change with C cycles for assessing carbon-climate feedback use constant Q_{10} values of ~ 2[10,11]. However, in contrast to modeling predictions, numerous field studies indicate variable Q_{10} with positive responses of soil respiration to warming declining over time[7,12-15]. The decreased temperature sensitivity in response to warming is termed acclimation[12].

89 The phenomenon of respiratory acclimation is of critical importance because it could weaken the
90 positive feedback between C cycle and climate warming[12]. It can be explained by two major
91 contrasting hypotheses: substrate depletion[5,7,15,16] and microbial adaptation[12]. The former
92 hypothesizes that soil labile C becomes depleted by the increased respiration in response to warming,
93 which leads to subsequent reduction in the rate of soil respiration. The latter hypothesizes that
94 respiratory acclimation results from the adaptive changes of microbial community structure[12,17].
95 These two contrasting hypotheses may lead to opposite consequences in terms of soil C dynamics
96 and global warming[7]. If the reduced temperature sensitivity of soil respiration under warming is due
97 to changes in microbial community structure, then relatively more C may still be preserved in soils
98 under warming than in the scenario of non-acclimation or acclimation induced by substrate limitation.
99 This may diminish the positive feedback between C cycling and climate warming. However, if the
100 substrate limitation is the main reason for the reduced temperature sensitivity of soil respiration, the
101 increased plant-derived C under warming will exacerbate the positive feedback by releasing more C
102 into the atmosphere through soil respiration. Therefore, understanding the mechanisms underlying
103 the respiratory acclimation phenomenon is critical to improving the quantitative framework of
104 carbon-climate models and hence to projecting future climate warming.
105 To determine whether substrate limitation contributes to the decreased temperature sensitivity,
106 total soil organic C and labile C were measured and the recalcitrant C was calculated for soils
107 collected in 2008. Three strong points of evidence indicated that the decreased temperature
108 sensitivity of soil respiration was not due to substrate depletion. (**i**). The labile C (labile C pool 1 plus
109 labile C pool 2) was slightly (7.2%) higher in warmed plots than control plots (Fig 1B) although they
110 were not statistically different. Warming significantly increased soil labile C for samples collected in
111 2002[18]. If substrate depletion is the main factor, one would have expected that the labile C content
112 would be substantially lower under warming. Thus, this strongly suggests that C substrate is not
113 depleted under warming, or at least that the substrate may not be more limited in warmed plots than
114 in control plots. (**ii**). If the substrate is depleted under warming, microbial biomass would have been
115 expected to decrease. However, the microbial biomass measured by phospholipid fatty acid (PLFA)
116 analysis in 2008 was significantly higher under warming (Fig. 1C). (**iii**) The bacterial and fungal

abundances based on GeoChip were marginally significantly higher by a one-tailed paired t test under warming than in the control, which also implies that C substrate might be not limited under warming. Overall, the above results implied that the decreased temperature sensitivity of soil respiration was not due to substrate depletion, but likely attributed to the changes in microbial community composition and structure though further studies will be required to confirm it and establish a mechanistic link.

4. **Fungi/bacteria biomass**

A previous study examined the bacterial and fungal biomass based on a phospholipid fatty acids (PLFAs) profile[19]. Three fatty acids (16:1ω5c, 18:2ω6.9c and 18:1ω9c) were selected to represent the fungal group. For all three sampling points, warming did not affect the bacteria or fungal biomass significantly. However, its interaction with clipping was a significant factor for bacteria and fungi biomass in September, 2001 and 2002, respectively[19], and for the ratio between fungi and bacteria biomass in both years. Without clipping, the ratio between fungal and bacterial biomass was significantly higher under warming than in the control[21] (Fig.4 in that paper). Based on these data, the authors concluded that warming induced microbial community to shift towards a higher fungal biomass. However, in this study, no such shifts towards more abundant fungi were observed as indicated by three complementary analyses: (**i**) PLFAs, (**ii**) GeoChip hybridization abundance signals, and (**iii**) soil enzyme activities (Fig 1).

There are two main possible reasons to explain this discrepancy. One is that the shift of microbial communities to fungi observed in 2001 could be transient. Also, it could be due to methodological differences. One of the fatty acids used (16:1ω5c) is not specific to fungi and has been used as a signature for bacteria in some studies[20,21]. Since the fatty acid, 18:2ω6.9c, was not detected in our study, only a single fatty acid (18:1ω9c) was used. Such methodological differences could contribute to the discrepancy observed between these two studies. Since three different but complementary approaches were used to estimate fungal abundance and activities in this study (see above), we believe that the conclusion drawn in this study should be reliable.

5. Phosphorus utilization

Phosphorus is an essential plant nutrient. GeoChip has many probes derived from the genes involved in phosphorus utilization. Our analysis showed that the key gene encoding polyphosphate kinase involved in phosphorus utilization increased significantly under warming (Fig. S8). These results are also consistent with the general notion that warming enhances nutrient cycling[6].

Reference

1. A. Ramette, J. M. Tiedje, *Proc. Natl. Acad. Sci. U.S.A.* **104**, 2761 (2007).
2. Y. Liang *et al.*, *ISME J.* **5**, 403 (2011).
3. J. Zhou, S. Kang, C. W. Schadt, C. T. Garten, Jr., *Proc. Natl. Acad. Sci. U.S.A.* **105**, 7768 (2008).
4. E. A. Davidson, I. A. Janssens, *Nature* **440**, 165 (2006).
5. W. Knorr, I. C. Prentice, J. I. House, E. A. Holland, *Nature* **433**, 298 (2005).
6. Y. Q. Luo, *Annu. Rev. Ecol. Evol. Syst.***38**, 683 (2007).
7. I. P. Hartley, A. Heinemeyer, P. Ineson, *Global Change Biol.* **13**, 1761 (2007).
8. K. Maseyk, J. M. Grunzweig, E. Rotenberg, D. Yakir, *Global Change Biol.* **14**, 1553 (2008).
9. P. Vanhala *et al.*, *Soil Biol. Biochem.* **40**, 1758 (2008).
10. P. M. Cox, R. A. Betts, C. D. Jones, S. A. Spall, I. J. Totterdell, *Nature* **408**, 184 (2000).
11. P. Friedlingstein *et al.*, *J. Clim.* **19**, 3337 (2006).
12. Y. Q. Luo, S. Q. Wan, D. F. Hui, L. L. Wallace, *Nature* **413**, 622 (2001).
13. L. E. Rustad *et al.*, *Oecologia* **126**, 543 (2001).
14. J. M. Melillo *et al.*, *Science* **298**, 2173 (2002).
15. M. U. F. Kirschbaum, *Global Change Biol.* **10**, 1870 (2004).
16. L. H. Gu, W. M. Post, A. W. King, *Global Biogeochem. Cycles* **18**, (2004).
17. B. M. Gema, G. B. Maria, R. Johannes, B. Erland, *Global Change Biol.* **15**, 2950 (2009).
18. A. Belay-Tedla, X. H. Zhou, B. Su, S. Q. Wan, Y. Q. Luo, *Soil Biol. Biochem.* **41**, 110 (2009).
19. W. Zhang *et al.*, *Global Change Biol.* **11**, 266 (2005).
20. J. R. Vestal, D. C. White, *Biosci.* **39**, 535 (1989).
21. E. Baath, A. Frostegard, H. Fritze, *Appl. Environ. Microb.* **58**, 4026 (1992).